



Published in final edited form as:

*Bioorg Med Chem Lett.* 2022 November 15; 76: 129013. doi:10.1016/j.bmcl.2022.129013.

## Structure-activity relationship studies in a new series of 2-amino-*N*-phenylacetamide inhibitors of Slack potassium channels

Alshaima'a M. Qunies<sup>a,b,1</sup>, Nigam M. Mishra<sup>a,1</sup>, Brittany D. Spitznagel<sup>c</sup>, Yu Du<sup>c,d</sup>, Valerie S. Acuña<sup>a</sup>, C. David Weaver<sup>c,d</sup>, Kyle A. Emmitte<sup>a,\*</sup>

<sup>a</sup>Department of Pharmaceutical Sciences, UNT System College of Pharmacy, University of North Texas Health Science Center, Fort Worth, TX USA

<sup>b</sup>Graduate School of Biomedical Sciences, University of North Texas Health Science Center, Fort Worth, TX USA

<sup>c</sup>Department of Pharmacology, Vanderbilt University, Nashville, TN 37232 USA

<sup>d</sup>Vanderbilt Institute of Chemical Biology, Vanderbilt University, Nashville, TN 37232 USA

### Abstract

In this Letter we describe structure-activity relationship (SAR) studies conducted in five distinct regions of a new 2-amino-*N*-phenylacetamides series of Slack potassium channel inhibitors exemplified by recently disclosed high-throughput screening (HTS) hit VU0606170 (4). New analogs were screened in a thallium (Tl<sup>+</sup>) flux assay in HEK-293 cells stably expressing wild-type human (WT) Slack. Selected analogs were screened in Tl<sup>+</sup> flux versus A934T Slack and other Slo family members Slick and Maxi-K and evaluated in whole-cell electrophysiology (EP) assays using an automated patch clamp system. Results revealed the series to have flat SAR with significant structural modifications resulting in a loss of Slack activity. More minor changes led to compounds with Slack activity and Slo family selectivity similar to the HTS hit.

### Keywords

Slack; K<sub>Na</sub>1.1; Slo2.2; *KCNT1*; MMPSI; EIMFS; 2-amino-*N*-phenylacetamide

Malignant migrating partial seizure of infancy (MMPSI), also known as epilepsy of infancy with migrating focal seizures (EIMFS), is a rare, serious form of infantile epilepsy.<sup>1</sup> Patients with MMPSI are typically pharmacoresistant with seizure onset developing within the first six months of life and a 25% mortality rate within the first year. Approximately half of MMPSI cases have been linked to multiple *de novo* gain-of-function (GOF) heterozygous missense mutations in the *KCNT1* gene.<sup>2,3</sup> *KCNT1* encodes for the sodium-activated potassium channel known as K<sub>Na</sub>1.1 or Slack (Sequence Like A Calcium-Activated K<sup>+</sup>

\*Corresponding author. kyle.emmitte@unthsc.edu.

<sup>1</sup>A. M. Qunies and N. M. Mishra contributed equally to this work

Supporting Information

Synthetic chemistry and pharmacological methods associated with this article can be found in the Supporting information.

Channel). Slack is a member of the Slo family (Slo2.2) of K<sup>+</sup> channels along with Slo1 (Maxi-K), Slo2.1 (Slick), and Slo3. Slack channels are essential regulators of electrical activity and distributed throughout the central nervous system, where they play important roles in affecting neuronal excitability.<sup>3–7</sup> Slack channels are characterized by 4 subunits with six hydrophobic transmembrane domains (S1–S6) and a pore-forming domain between S5 and S6. Also present are an extended C-terminal cytoplasmic domain, containing a regulator of potassium conductance (RCK) domain and a nicotinamide adenine dinucleotide-binding (NAD<sup>+</sup>) domain.<sup>2, 6, 8–11</sup>

Several recent reports have documented more than 30 mutations in Slack. The GOF mutations correlated with MMPSI are associated with an increase in Slack current.<sup>3, 12–15</sup> In addition to MMPSI, *KCNT1* GOF mutations are associated with other epilepsy disorders, including autosomal dominant sleep-related hypermotor epilepsy (ADSHE),<sup>16</sup> early-onset epileptic encephalopathy (EOEE),<sup>17</sup> myoclonic-atonic epilepsy,<sup>18</sup> temporal lobe epilepsy with intellectual disability,<sup>19</sup> and autosomal dominant nocturnal frontal lobe epilepsy (ADNFLE).<sup>20, 21</sup> Multiple potential mechanisms by which these GOF mutations in Slack channels lead to increased neuronal excitability and rate of firing have been put forth. For example, activation of Slack channels leads to increased amplitude of AHP, resulting in shorter action potentials and increased neuronal firing frequency.<sup>12, 22</sup> Likewise, GOF Slack mutations may reduce the excitability of inhibitory interneurons, ultimately leading to decreased inhibitory tone.<sup>8, 13</sup> Finally, Slack also has non-conducting functions, and interacts with downstream signaling pathways that may be disrupted by mutations.<sup>22, 23</sup>

No broadly effective and safe drug therapy option is presently available for the treatment of MMPSI. Drugs such as quinidine, bepridil, and cofilium modulate Slack currents *in vitro*, and attempts have been made to repurpose them for *KCNT1*-associated epilepsies; however, these compounds are hampered by a lack of selectivity, toxicity, and suboptimal drug metabolism and pharmacokinetic (DMPK) properties.<sup>4, 8, 14, 24–30</sup> Notably, recent reports have described new compounds from diverse chemotypes that inhibit Slack function (Figure 1).<sup>31</sup> For example, virtual screening of a commercial library employing a cryo-electron microscopy-derived structure of chicken K<sub>Na</sub>1.1 identified six Slack inhibitors with micromolar potency, each one predicted to function via blockade of the channel pore.<sup>32</sup> Compounds **1–2** are representative analogs with reported IC<sub>50</sub> values of 3.2 and 3.0 μM, respectively, in a whole-cell patch clamp assay using HEK-293 cells expressing human wild-type (WT) Slack channels. In addition, a high-throughput screen (HTS) and ensuing optimization effort identified orally available 1,2,4-oxadiazole **3**, which normalizes the EEG phenotype in a mouse model of *Kcnt1* GOF.<sup>33</sup> Compound **3** was a potent Slack inhibitor with a reported IC<sub>50</sub> of 40 nM in an automated patch clamp assay in HEK-TREX cells stably expressing human WT Slack channels. Finally, we recently reported the results of our own HTS utilizing a thallium (Tl<sup>+</sup>) flux assay in HEK-293 cells stably expressing human WT and selected mutant Slack channels. The 2-amino-*N*-phenylacetamide VU0606170 (**4**) was identified through this campaign and possessed low micromolar potency for both WT and A934T Slack in Tl<sup>+</sup> flux and whole-cell automated patch-clamp assays. VU0606170 (**4**) has an attractive selectivity profile and decreased the firing rate in an overexcited, spontaneously firing cortical neuronal culture consistent with an antiepileptic effect.<sup>34</sup> In

this Letter, we report the results of structure-activity relationship (SAR) studies within the 2-amino-*N*-phenylacetamide chemotype exemplified by **4**.

Desiring to rapidly evaluate the potential tractability of VU0606170 (**4**), we decided to pursue SAR development in five regions of the scaffold (Figure 2). Where amenable, we employed late-stage penultimate intermediates that facilitated the synthesis of small compound libraries. Scheme 1 was used to evaluate SAR in the eastern ring of the scaffold. Commercial sulfamoyl chloride **5** was reacted with 1-Boc-piperazine **6** to afford sulfamide **7**. Cleavage of the protecting group under acidic conditions gave secondary amine **8** as the trifluoroacetic acid salt. Alkylation of **8** with ethyl bromoacetate was accomplished with mild heating to provide ester **9**. Hydrolysis of the ester with aqueous lithium hydroxide afforded acid and penultimate intermediate **10**. Coupling with a variety of aryl amines provided final amide analogs **11-29** and **31-36**. Synthesis of analog **30** via amide coupling proved ineffective. Thus, 2,5-dichloroaniline **37** was alkylated with chloroacetyl chloride to afford **38**, which was subsequently reacted with intermediate **8** to provide **30**.

Screening of all new compounds versus WT Slack in our TI<sup>+</sup> flux assay utilized optimized buffer conditions that were slightly modified from those previously published to afford a larger signal amplitude (see Supporting Information).<sup>34</sup> An initial scan at all positions employing common functional groups quickly alerted us to the potential for mode switching in the scaffold as most of the analogs were weak activators of the channel (Table 1). Such an observation is consistent with compounds in this chemotype modulating Slack function by a mechanism other than simple pore blockade. A few analogs (**15**, **18**, **19**, and **22**) displayed a mixed profile, appearing to behave as either weak inhibitors or inactive at higher concentrations and weak activators at low concentrations. Although the reason for this profile is not known, a possible explanation is that there are two binding sites in the channel and occupancy of the first site is weakly activating while occupancy of both is inhibiting. Alternatively, there may be two distinct binding sites, one activating and the other inhibiting. Given that 2-methoxy analog **21** was the only compound that maintained the inhibitory profile observed with VU0606170 (**4**), we redirected our efforts toward analogs that maintained the 2,5-disubstituted pattern of **4** with either the 2-methoxy group (**24-28**) or the 5-chloro group (**29-35**) held constant (Table 2).

Replacement of the 5-chloro group with other electron-withdrawing substituents maintained the inhibitory profile with bromo (**25**) and trifluoromethyl (**27**) analogs showing similar potency to VU0606170 (**4**). Notably, while the potency was similar, **25** demonstrated approximately half of the efficacy observed with **4** and **27** as evidenced by clear plateauing of the CRC well above the maximum observed with the control compound. Replacement of the 2-methoxy group with halogens (**29** and **30**) or methyl (**31**) was not effective. Analogs **32-35** explored lengthening and branching of the alkyl ether substituent. In each case, the compounds were inhibitors; however, potency was 2–3 fold lower than **4**. Finally, analog **36** demonstrated the lack of tolerance for an aromatic nitrogen atom.

To explore SAR in the western ring and associated linker 1, we employed chemistry outlined in Scheme 2. Reaction of 1-Boc-piperazine **6** with ethyl bromoacetate under basic conditions afforded ester **39**. Hydrolysis of the ester with lithium hydroxide provided lithium salt

intermediate **40**. Coupling of **40** with 5-chloro-2-methoxyaniline proceeded with HATU. Removal of the Boc protecting group gave secondary amine **42** as its trifluoroacetic acid salt. Reaction of **42** with sulfamoyl chlorides provided sulfamides **43** and **44**, while reaction with sulfonyl chlorides yielded sulfonamides **45-48**. To access urea analogs **50-55**, we first converted **42** to 4-nitrophenylcarbamate **49**. Treatment of **49** with various cyclic secondary amines under microwave heating afforded the desired ureas **50-55**.<sup>35</sup>

The most modest changes in the western ring (**43-45**) were not tolerated (Table 3). Benzene and 4-chlorobenzene sulfonamides **46** and **48** exhibited potency on par with **4**; however, efficacy was diminished considerably. Surprisingly, 4-methylbenzene sulfonamide **47** was inactive. For the most part, the urea analogs were weak activators of the channel (**50**, **51**, **54**, and **55**) or displayed a mixed profile (**53**). Only analog **52** functioned as a weak inhibitor.

We previously reported that relocation of the carbonyl group on linker 2 from the carbon adjacent to the aniline nitrogen to the carbon adjacent to the piperazine nitrogen was not tolerated.<sup>34</sup> In fact, we employed this regioisomer of VU0606170 known as VU0849686 as a negative control. Still, we were interested in exploring substitution of the linker and investigated stereospecific methylated analogs via Scheme 3. Following a method described in the patent literature,<sup>36</sup> we converted commercially available chiral alcohol **56** to its corresponding triflate **57**, which was reacted with secondary amine **8** to provide **58** with inversion of stereochemistry. Hydrolysis of the methyl ester was accomplished with 6N hydrochloric acid and heating to provide acid **59** as its hydrochloride salt. Coupling with 5-chloro-2-methoxyaniline and 2-methoxy-5-(trifluoromethyl)aniline afforded analogs **60** and **61**, respectively. The same sequence was repeated utilizing methyl (*S*)-2-hydroxypropanoate instead of **56** to afford the *R*-enantiomer analogs **62** and **63** (Table 4). No evidence of significant preference for one enantiomer versus the other was noted. In both cases the trifluoromethyl analogs (**61** and **63**) were slightly more potent than the chloro analogs (**60** and **62**); however, all four compounds were 1.5 to 2-fold less potent than the hit VU0606170 (**4**).

In the core of the scaffold, we sought to evaluate the impact of substitution as well as the tolerability for various piperazine isosteres.<sup>35, 37, 38</sup> In some cases the core monomers were not symmetric (e.g., **64** in Scheme 4), and we thus employed complementary routes to arrive at two distinct analogs. Specifically, monomer **64** was converted to sulfamide **65** as described previously. Removal of the protecting group to afford **66** and subsequent alkylation with **67** gave analog **68**. The same three-step sequence was also carried out in reverse order to arrive at analog **71**. The same complementary approach was likewise followed for monomers **72** and **73**, while symmetric monomers **74-76** were simply reacted in the manner used to prepare analog **71**. Two additional core analogs (**80** and **85**) followed slightly modified procedures (Scheme 5). In the case of acyclic analog **80**, the use of a protecting group was avoided by employing an excess of diamine **77**. The remaining steps were as previously described. Preparation of piperidine analog **85** utilized previously outlined chemistry but was initiated with starting material **82**, which already contained an ester group.

Methyl substitution of the piperazine core on the carbon adjacent to the sulfamide nitrogen (**68** and **86**) significantly reduced potency (Table 5). On the other hand, methyl substitution of the other carbon was well tolerated (**71** and **87**), with (*R*)-enantiomer **87** being equipotent to hit compound **4**. Acyclic analog **81** retained inhibitory activity but exhibited reduced potency, likely due to increased degrees of rotational freedom. Piperidine **85** and spirocycles **88** and **89** were weak activators while spirocycle **90** was a weak inhibitor. Octahydropyrrolo[3,4-*c*]pyrrole **91** was the only analog in this set devoid of activity at Slack. Finally, expansion of the ring in the form of homopiperazine **92** gave a moderately potent analog.

Our SAR studies in the VU0606170 (**4**) chemotype to date have not identified analogs that improve upon the potency of the hit compound. Still, we have identified several analogs that were equipotent or near equipotent with **4**.<sup>8</sup> Thus, we decided to take a closer look at the pharmacological profiles of select analogs. First, we screened nine select inhibitors against A934T mutant Slack, a variant commonly associated with MMPSI (Table 6).<sup>2, 3</sup> All of the molecules functioned as inhibitors and were equipotent or more potent versus A934T as compared to WT with the majority of the molecules being slightly more potent versus A934T. Such a result may indicate that our inhibitors block an open confirmation of the channel, a phenomena observed with quinidine in other variants with Slack GOF mutations.<sup>8</sup>

We next chose three of the most potent inhibitors with variations at distinct points of the scaffold for screening versus Slick (Slo2.1) and Maxi-K (Slo1  $\alpha 1/\beta 3$ ) to assess Slo family selectivity (Table 7). Selectivity versus Maxi-K was generally very good, with **27** and **87** showing weak inhibition and **61** being inactive. Most analogs demonstrated weak inhibition of Slick. While **27** had an IC<sub>50</sub> of 4.1  $\mu$ M, efficacy was low at 29% of the positive control. Thus, these analogs displayed similar selectivity to VU0606170 (**4**), which is not surprising, given the small structural differences. These same three inhibitors were also examined in a whole-cell electrophysiology (EP) assays using an automated patch clamp system (SyncroPatch 384) (Table 8). Gratifyingly, potency and efficacy in this assay was on par with those observed in TI<sup>+</sup> flux in both WT and A934T expressing cells with each of these analogs.

In conclusion, we have executed SAR studies in a new series of 2-amino-*N*-phenylacetamide inhibitors of Slack potassium channels based on the HTS hit VU0606170. Systematic evaluation of five distinct regions of the chemotype revealed flat SAR with most substantial structural modifications proving deleterious to Slack activity. Some analogs with more modest structural deviations from the hit compound exhibit potency on par with the HTS hit. For example, chiral methyl substituents on the core (**87**) and linker 2 (**61**) and exchange of the chloro group of the hit for a trifluoromethyl group (**27** and **61**) gave potent analogs. Importantly, testing of selected analogs versus the A934T Slack mutant revealed potency on par with the WT, and results in whole-cell EP mirrored those obtained with TI<sup>+</sup> flux for the same analogs, validating our primary optimization screening approach utilizing TI<sup>+</sup> flux as our frontline assay. Utilization of homology models and docking studies might prove instrumental in the optimization of small molecule Slack inhibitors in the future; however, additional information about the binding site for these compounds would be required to best enable such an approach. The observed mode-switching in this scaffold argues against the

compounds functioning as simple pore blockers. Hit evaluation and optimization continues in additional distinct scaffolds discovered through our HTS campaign. Reports from those efforts will be reported in the near future.

## Supplementary Material

Refer to Web version on PubMed Central for supplementary material.

## Acknowledgments

We thank the National Institute of Neurological Disorders and Stroke (R33NS109521 to C.D.W. and K.A.E.) for their support of our program in the development of small molecule inhibitors of Slack channels. Funding for the WaveFront Biosciences Panoptic kinetic imaging plate reader and the SyncroPatch 768 PE platform was provided by the Office of The Director (OD) of the National Institutes of Health under the award numbers 1S10OD021734 and 1S10OD021734, respectively.

## References and Notes

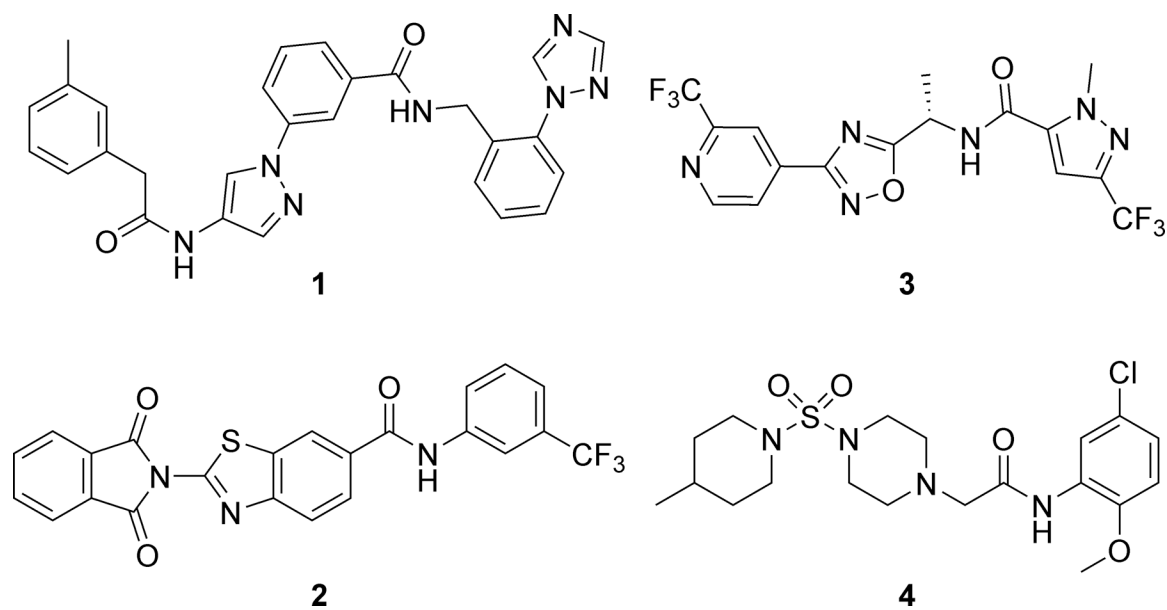
1. Coppola G, Plouin P, Chiron C, Robain O, Dulac O. Migrating partial seizures in infancy: a malignant disorder with developmental arrest. *Epilepsia* 1995;36(10): 1017–1024. [PubMed: 7555952]
2. McTague A, Nair U, Malhotra S, et al. Clinical and molecular characterization of *KCNT1*-related severe early-onset epilepsy. *Neurology* 2018;90(1): e55–e66. [PubMed: 29196579]
3. Barcia G, Fleming MR, Deligniere A, et al. De novo gain-of-function *KCNT1* channel mutations cause malignant migrating partial seizures of infancy. *Nat Genet* 2012;44(11): 1255–1259. [PubMed: 23086397]
4. Barcia G, Chemaly N, Kuchenbuch M, et al. Epilepsy with migrating focal seizures: *KCNT1* mutation hotspots and phenotype variability. *Neurology Genetics* 2019;5(6): e363. [PubMed: 31872048]
5. Yuan A, Santi CM, Wei A, et al. The sodium-activated potassium channel is encoded by a member of the Slo gene family. *Neuron* 2003;37(5): 765–773. [PubMed: 12628167]
6. Bhattacharjee A, Gan L, Kaczmarek LK. Localization of the Slack potassium channel in the rat central nervous system. *The Journal of comparative neurology* 2002;454(3): 241–254. [PubMed: 12442315]
7. Joiner WJ, Tang MD, Wang LY, et al. Formation of intermediate-conductance calcium-activated potassium channels by interaction of Slack and Slo subunits. *Nature neuroscience* 1998;1(6): 462–469. [PubMed: 10196543]
8. Rizzo F, Ambrosino P, Guacci A, et al. Characterization of two de novo *KCNT1* mutations in children with malignant migrating partial seizures in infancy. *Molecular and cellular neurosciences* 2016;72: 54–63. [PubMed: 26784557]
9. Kaczmarek LK. Slack, Slick and Sodium-Activated Potassium Channels. *International scholarly research notices* 2013;2013: Article ID 354262.
10. Zhang Z, Rosenhouse-Dantsker A, Tang QY, Noskov S, Logothetis DE. The RCK2 domain uses a coordination site present in Kir channels to confer sodium sensitivity to Slo2.2 channels. *J Neurosci* 2010;30(22): 7554–7562. [PubMed: 20519529]
11. Bhattacharjee A, Joiner WJ, Wu M, Yang Y, Sigworth FJ, Kaczmarek LK. Slick (Slo2.1), a rapidly-gating sodium-activated potassium channel inhibited by ATP. *J Neurosci* 2003;23(37): 11681–11691. [PubMed: 14684870]
12. Quraishi IH, Mercier MR, McClure H, et al. Impaired motor skill learning and altered seizure susceptibility in mice with loss or gain of function of the *Kcnt1* gene encoding Slack ( $K_{Na1.1}$  Na(+)-activated K(+) channels. *Sci Rep* 2020;10(1): 3213. [PubMed: 32081855]
13. Kim Grace E, Kronengold J, Barcia G, et al. Human Slack Potassium Channel Mutations Increase Positive Cooperativity between Individual Channels. *Cell reports* 2014;9(5): 1661–1672. [PubMed: 25482562]



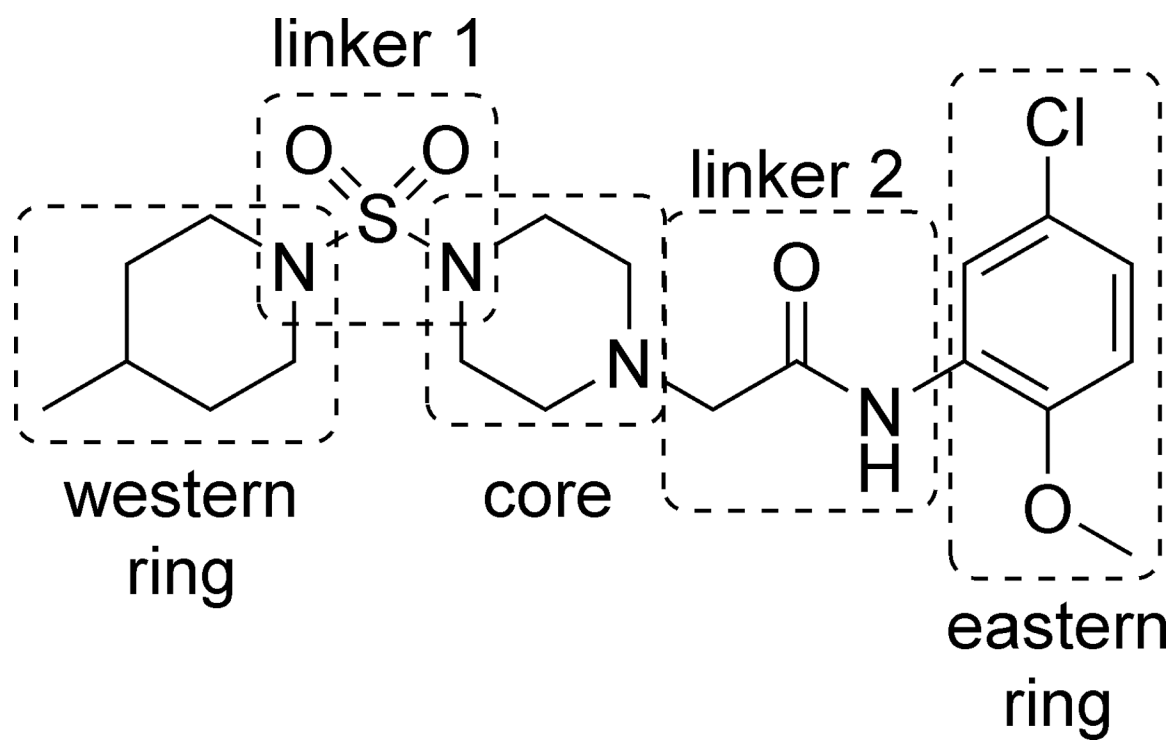
14. Milligan CJ, Li M, Gazina EV, et al. KCNT1 gain of function in 2 epilepsy phenotypes is reversed by quinidine. *Annals of neurology* 2014;75(4): 581–590. [PubMed: 24591078]
15. Martin HC, Kim GE, Pagnamenta AT, et al. Clinical whole-genome sequencing in severe early-onset epilepsy reveals new genes and improves molecular diagnosis. *Human molecular genetics* 2014;23(12): 3200–3211. [PubMed: 24463883]
16. Heron SE, Smith KR, Bahlo M, et al. Missense mutations in the sodium-gated potassium channel gene *KCNT1* cause severe autosomal dominant nocturnal frontal lobe epilepsy. *Nature Genetics* 2012;44(11): 1188–1190. [PubMed: 23086396]
17. Ohba C, Kato M, Takahashi N, et al. De novo *KCNT1* mutations in early-onset epileptic encephalopathy. *Epilepsia* 2015;56(9): e121–128. [PubMed: 26140313]
18. Routier L, Verny F, Barcia G, et al. Exome sequencing findings in 27 patients with myoclonic-astatic epilepsy: Is there a major genetic factor? *Clinical Genetics* 2019;96(3): 254–260. [PubMed: 31170314]
19. Hansen N, Widman G, Hattingen E, Elger CE, Kunz WS. Mesial temporal lobe epilepsy associated with KCNT1 mutation. *Seizure* 2017;45: 181–183. [PubMed: 28081520]
20. Borlot F, Abushama A, Morrison-Levy N, et al. *KCNT1*-related epilepsy: An international multicenter cohort of 27 pediatric cases. *Epilepsia* 2020.
21. Moller RS, Heron SE, Larsen LH, et al. Mutations in *KCNT1* cause a spectrum of focal epilepsies. *Epilepsia* 2015;56(9): e114–120. [PubMed: 26122718]
22. Quraishi IH, Stern S, Mangan KP, et al. An Epilepsy-Associated KCNT1 Mutation Enhances Excitability of Human iPSC-Derived Neurons by Increasing Slack KNa Currents. *J Neurosci* 2019;39(37): 7438–7449. [PubMed: 31350261]
23. Fleming MR, Brown MR, Kronengold J, et al. Stimulation of Slack K(+) Channels Alters Mass at the Plasma Membrane by Triggering Dissociation of a Phosphatase-Regulatory Complex. *Cell reports* 2016;16(9): 2281–2288. [PubMed: 27545877]
24. Yoshitomi S, Takahashi Y, Yamaguchi T, et al. Quinidine therapy and therapeutic drug monitoring in four patients with *KCNT1* mutations. *Epileptic disorders : international epilepsy journal with videotape* 2019;21(1): 48–54.
25. El Kousseifi C, Cornet M-C, Cilio MR. Neonatal Developmental and Epileptic Encephalopathies. *Seminars in Pediatric Neurology* 2019;32: 100770. [PubMed: 31813518]
26. Passey CC, Erramouspe J, Castellanos P, O'Donnell EC, Denton DM. Concurrent Quinidine and Phenobarbital in the Treatment of a Patient with 2 *KCNT1* Mutations. *Current therapeutic research, clinical and experimental* 2019;90: 106–108. [PubMed: 31388363]
27. Patil AA, Vinayan KP, Roy AG. Two South Indian Children with *KCNT1*-Related Malignant Migrating Focal Seizures of Infancy - Clinical Characteristics and Outcome of Targeted Treatment with Quinidine. *Annals of Indian Academy of Neurology* 2019;22(3): 311–315. [PubMed: 31359944]
28. Jia Y, Lin Y, Li J, et al. Quinidine Therapy for Lennox-Gastaut Syndrome With *KCNT1* Mutation. A Case Report and Literature Review. *Frontiers in neurology* 2019;10: 64. [PubMed: 30804880]
29. Dilena R, DiFrancesco JC, Soldovieri MV, et al. Early Treatment with Quinidine in 2 Patients with Epilepsy of Infancy with Migrating Focal Seizures (EIMFS) Due to Gain-of-Function *KCNT1* Mutations: Functional Studies, Clinical Responses, and Critical Issues for Personalized Therapy. *Neurotherapeutics : the journal of the American Society for Experimental NeuroTherapeutics* 2018;15(4): 1112–1126. [PubMed: 30112700]
30. Bearden D, Strong A, Ehnot J, DiGiovine M, Dlugos D, Goldberg EM. Targeted treatment of migrating partial seizures of infancy with quinidine. *Annals of neurology* 2014;76(3): 457–461. [PubMed: 25042079]
31. Qunies AM, Emmitte KA. Small-molecule inhibitors of Slack potassium channels as potential therapeutics for childhood epilepsies. *Pharmaceutical Patent Analyst* 2022;11(2): 45–56. [PubMed: 35369761]
32. Cole BA, Johnson RM, Dejakaisaya H, et al. Structure-Based Identification and Characterization of Inhibitors of the Epilepsy-Associated K(Na)1.1 (*KCNT1*) Potassium Channel. *iScience* 2020;23(5): 101100–101100. [PubMed: 32408169]

33. Griffin AM, Kahlig KM, Hatch RJ, et al. Discovery of the First Orally Available, Selective KNa1.1 Inhibitor: In Vitro and In Vivo Activity of an Oxadiazole Series. *ACS Medicinal Chemistry Letters* 2021;12(4): 593–602. [PubMed: 33859800]
34. Spitznagel BD, Mishra NM, Qunies AM, et al. VU0606170, a Selective Slack Channels Inhibitor, Decreases Calcium Oscillations in Cultured Cortical Neurons. *ACS Chemical Neuroscience* 2020;11(21): 3658–3671. [PubMed: 33143429]
35. Manka JT, Rodriguez AL, Morrison RD, et al. Octahydropyrrolo[3,4-*c*]pyrrole negative allosteric modulators of mGlu<sub>1</sub>. *Bioorg Med Chem Lett* 2013;23(18): 5091–5096. [PubMed: 23932792]
36. Åstrand ABM, Grimster NP, Kawatkar S, et al. , inventors; AstraZeneca AB, assignee. Compounds and methods for inhibiting JAK. *PCT Int. Patent Appl WO 2017/050938 A1*. 2017 Mar 30.
37. Melancon BJ, Utley TJ, Sevel C, et al. Development of novel M1 antagonist scaffolds through the continued optimization of the MLPCN probe ML012. *Bioorg Med Chem Lett* 2012;22(15): 5035–5040. [PubMed: 22749871]
38. Lachance N, Gareau Y, Guiral S, et al. Discovery of potent and liver-targeted stearoyl-CoA desaturase (SCD) inhibitors in a bispyrrolidine series. *Bioorg Med Chem Lett* 2012;22(2): 980–984. [PubMed: 22209206]

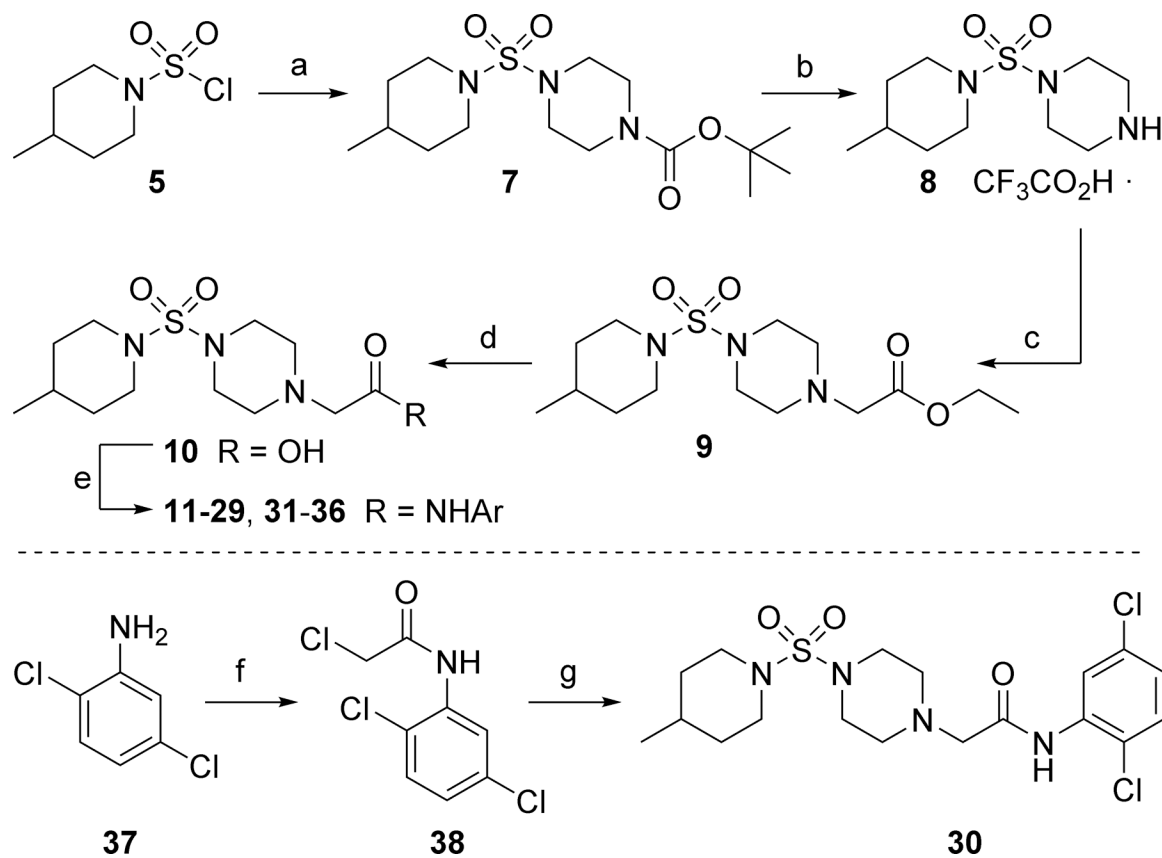




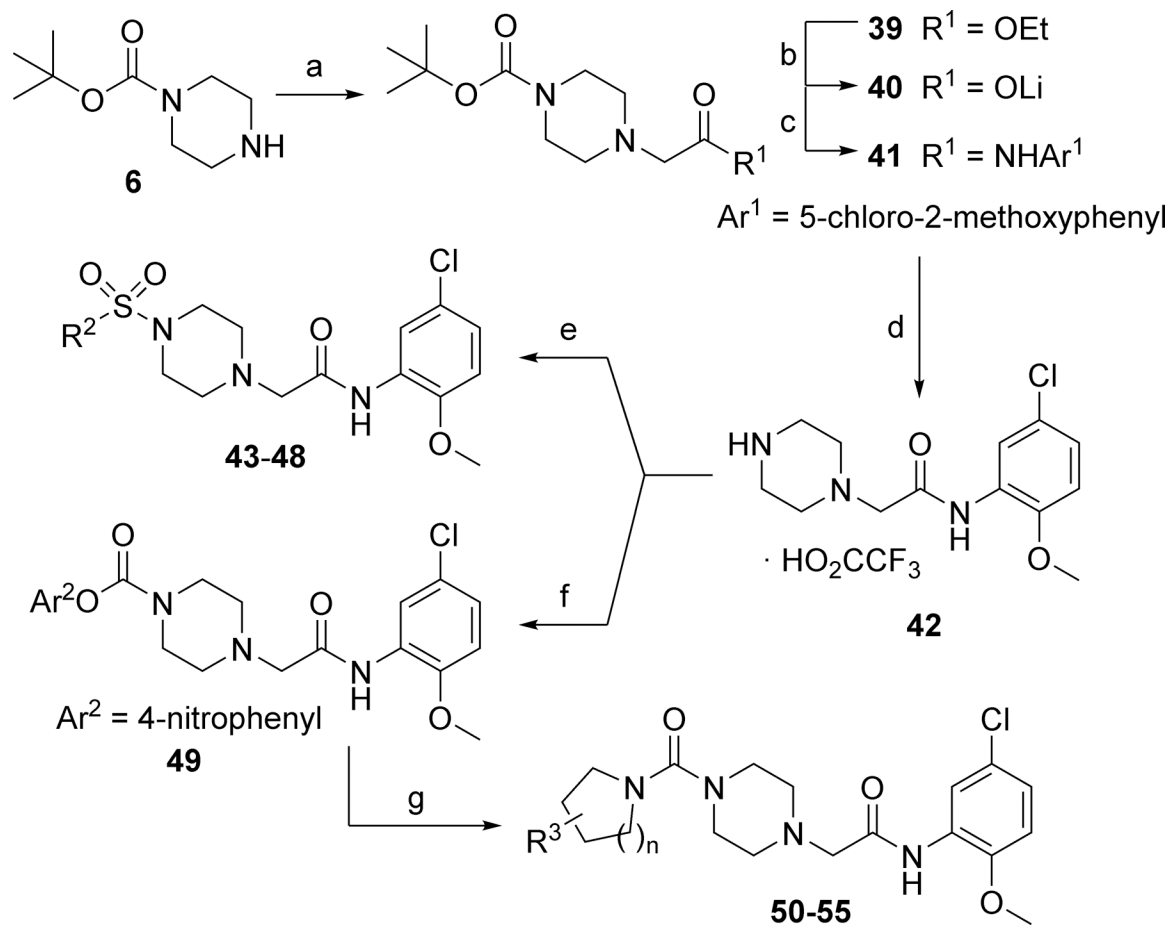
**Figure 1.** Recently reported small molecule inhibitors of Slack channels: predicted pore blockers **1-2**, *in vivo* tool **3**, and HTS hit **4** (VU0606170).



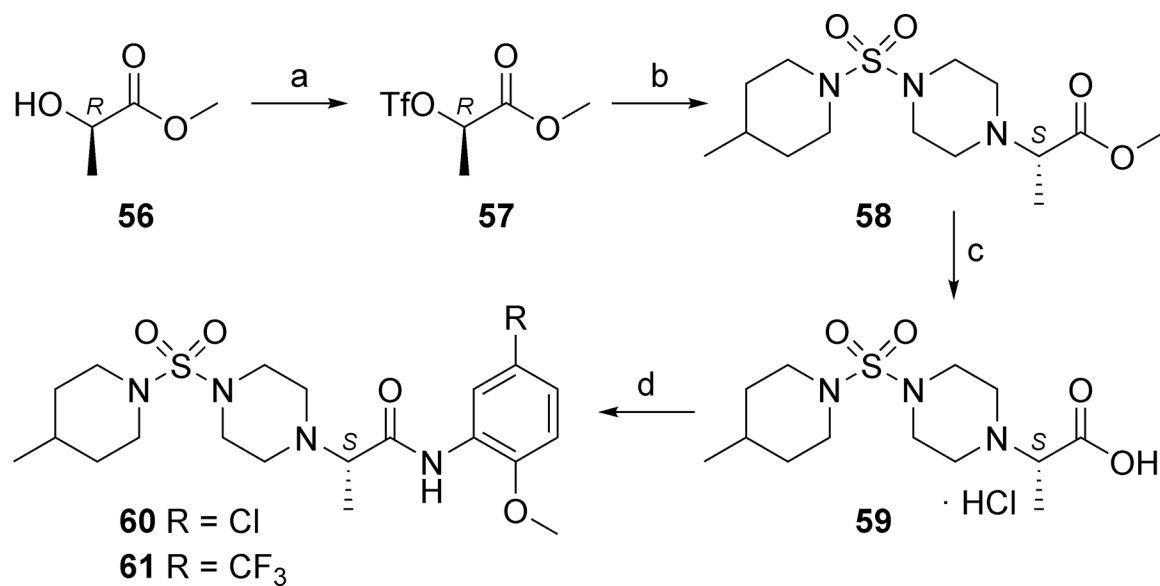
**Figure 2.**  
Regions for SAR development in the VU0606170 scaffold.

**Scheme 1.**

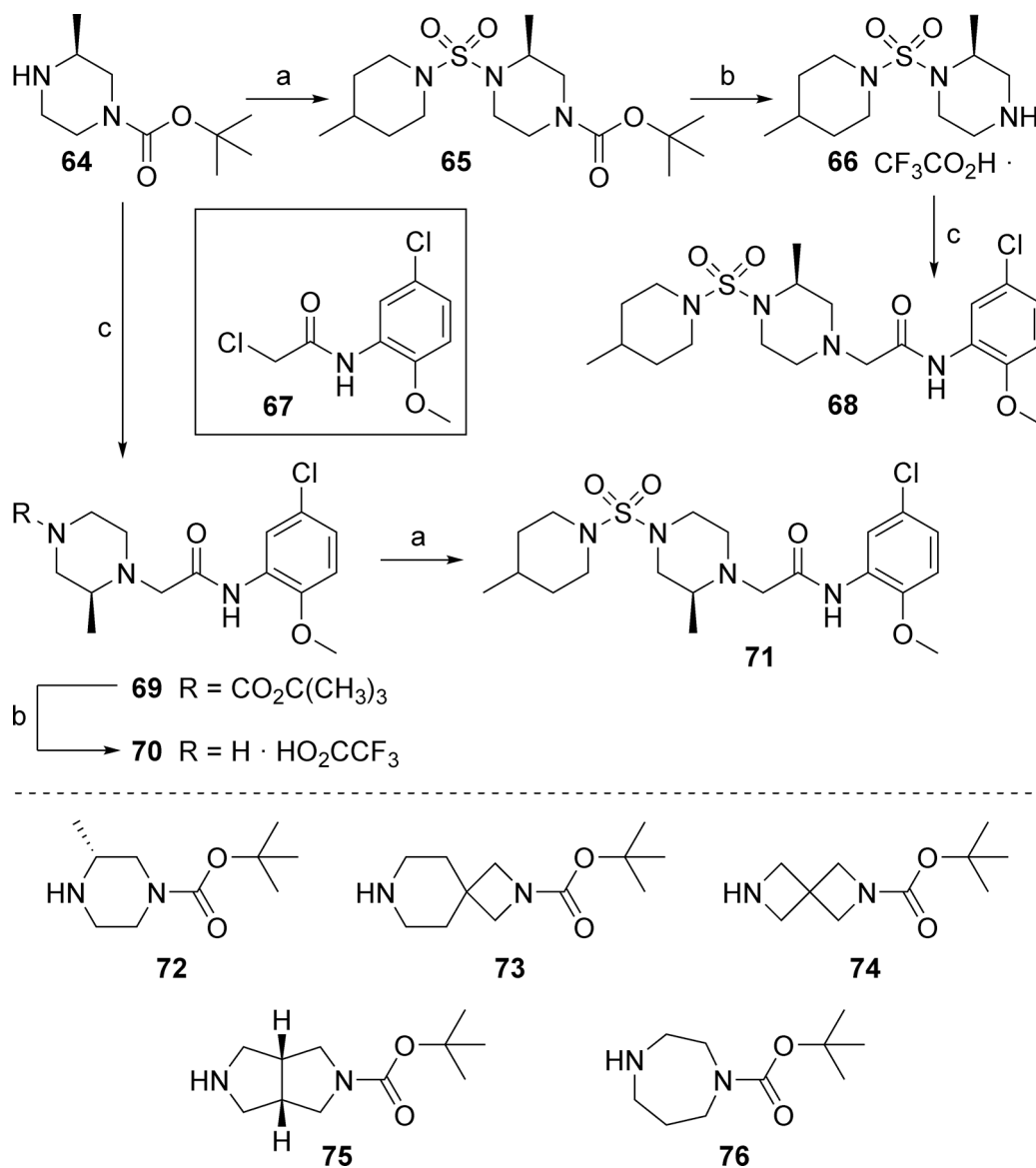
Reagents and conditions: (a) 1-Boc-piperazine (**6**), DIEA,  $\text{CH}_2\text{Cl}_2$ , 81%; (b) TFA,  $\text{CH}_2\text{Cl}_2$ , 97%; (c) Ethyl bromoacetate,  $\text{K}_2\text{CO}_3$ , DMF, 40 °C, 92%; (d) LiOH,  $\text{H}_2\text{O}$ , THF, 99%; (e)  $\text{ArNH}_2$ , HATU, DIEA, DMF, 4–64%; (f) chloroacetyl chloride,  $\text{NEt}_3$ , DMAP,  $\text{CH}_2\text{Cl}_2$ ; (g) **8**,  $\text{K}_2\text{CO}_3$ , KI, DMF, 50 °C, 7% (2 steps).

**Scheme 2.**

Reagents and conditions: (a) Ethyl bromoacetate,  $\text{K}_2\text{CO}_3$ , DMF, 68%; (b) LiOH,  $\text{H}_2\text{O}$ , THF, 98%; (c) 5-chloro-2-methoxyaniline, HATU, DIEA, DMF, 61%; (d) TFA,  $\text{CH}_2\text{Cl}_2$ , 100%; (e)  $\text{R}^2\text{SO}_2\text{Cl}$ , DIEA,  $\text{CH}_2\text{Cl}_2$ ; 41–58%; (f) 4-nitrophenyl chloroformate,  $\text{CH}_2\text{Cl}_2$ , 0 °C; (g) cyclic secondary amine, NMP,  $\mu\text{wave}$ , 200 °C, 25 min, 32–51% (2 steps).

**Scheme 3.**

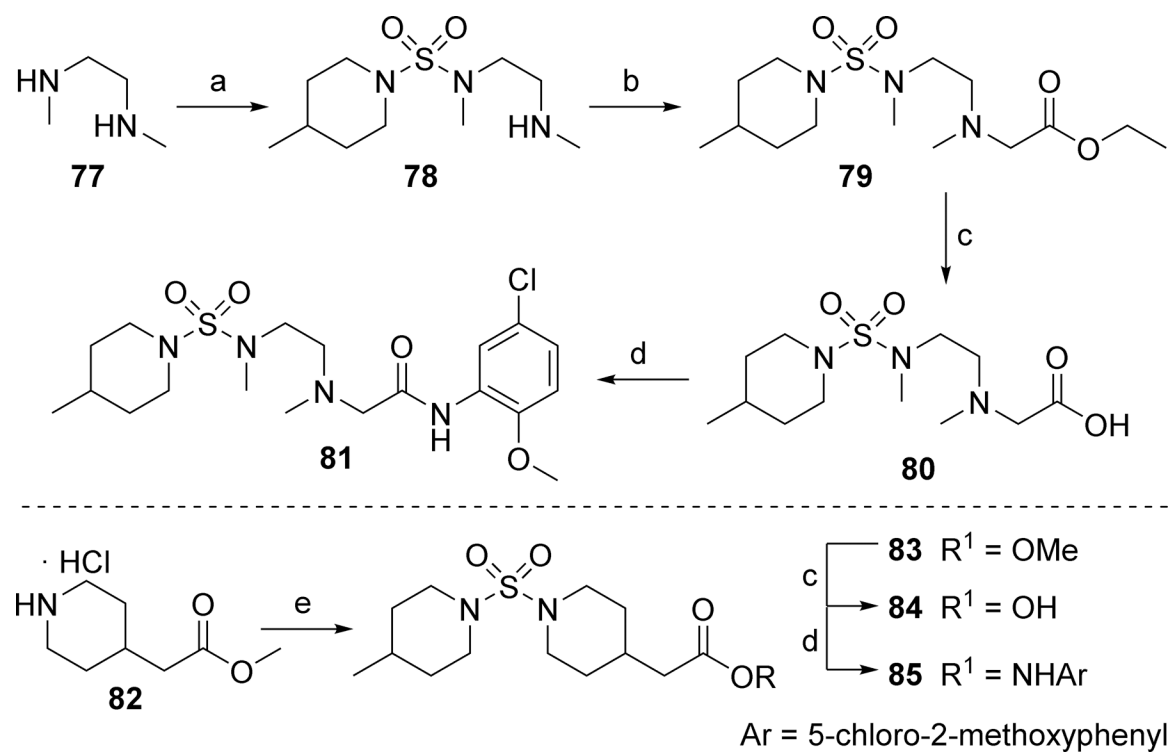
Reagents and conditions: (a) Tf<sub>2</sub>O, 2,6-lutidine, CH<sub>2</sub>Cl<sub>2</sub>, -70 °C to r.t., 53%; (b) **8**, K<sub>2</sub>CO<sub>3</sub>, CH<sub>2</sub>Cl<sub>2</sub>, H<sub>2</sub>O, 0 °C to r.t., 71%; (c) 6N HCl, 100 °C, 56%; (d) 5-chloro-2-methoxyaniline or 2-methoxy-5-(trifluoromethyl)aniline, HATU, DIEA, DMF, 35% (**60**), 63% (**61**).



**Scheme 4.**

Reagents and conditions: (a) **5**, DIEA,  $\text{CH}_2\text{Cl}_2$ , 61% (**65**), 98% (**71**); (b) TFA,  $\text{CH}_2\text{Cl}_2$ , 96% (**66**), 94% (**70**); (c) **67**, DIEA,  $\text{CH}_3\text{CN}$ , 75 °C, 66% (**68**), 81% (**69**).

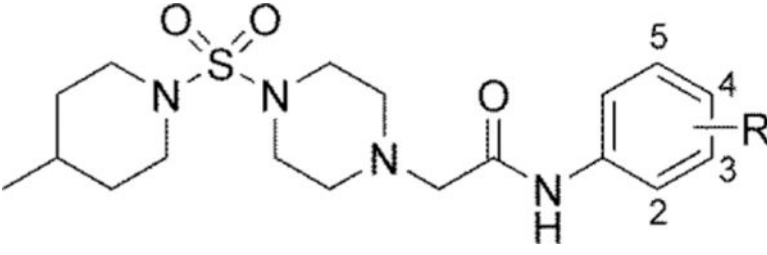


**Scheme 5.**

Reagents and conditions: (a) **5**, CH<sub>2</sub>Cl<sub>2</sub>, 99%; (b) Ethyl bromoacetate, K<sub>2</sub>CO<sub>3</sub>, DMF, 33%;  
 (c) LiOH, H<sub>2</sub>O, THF, 95% (**80**), 99% (**84**); (d) 5-chloro-2-methoxyaniline, HATU, DIEA,  
 DMF, 40% (**81**), 24% (**85**); (e) **5**, DIEA, CH<sub>2</sub>Cl<sub>2</sub>, 93%.

Table 1.

Eastern amide analogs from initial scan



No.	R	Mode <sup>a</sup>	IC <sub>50</sub> / EC <sub>50</sub> (μM) <sup>b</sup>	Efficacy (%) <sup>b,c</sup>
4	2-OMe, 5-Cl	Inh	2.4	100
11	H	Act	>10 <sup>d</sup>	21
12	2-F	Act	>10 <sup>d</sup>	30
13	3-F	Act	4.6	13
14	4-F	Act	>10 <sup>d</sup>	30
15	2-Cl		not determined <sup>e</sup>	
16	3-Cl	Act	7.6	38
17	4-Cl	Act	>10 <sup>d</sup>	58
18	2- Me		not determined <sup>e</sup>	
19	3- Me		not determined <sup>e</sup>	
20	4- Me	Act	4.1	13
21	2-OMe	Inh	>10 <sup>d</sup>	85
22	3-OMe		not determined <sup>e</sup>	
23	4-OMe	Act	>10 <sup>d</sup>	15

<sup>a</sup>Inh = inhibitor; Act = activator; NA = not active<sup>b</sup>Concentration-response curve (CRC) from Tl<sup>+</sup> flux assay in HEK-293 cells expressing WT Slack<sup>c</sup>Amplitude of response in the presence of 30 μM test compound as a percentage of the maximum response for VU0606170 (inhibitors) or loxapine (activators)<sup>d</sup>CRC does not plateau within the concentration range tested<sup>e</sup>Compounds appear to be weak inhibitors/inactive at high concentrations and weak activators at low concentrations

Table 2.

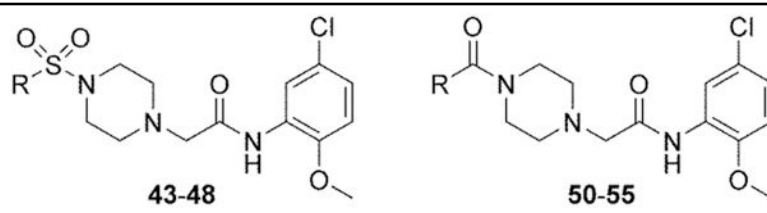
Eastern amide analogs from focused scan

No.	R	Mode <sup>a</sup>	IC <sub>50</sub> / EC <sub>50</sub> (μM) <sup>b</sup>	Efficacy (%) <sup>b,c</sup>
24	F	Inh	4.9	102
25	Br	Inh	1.4	52
26	Me	Inh	>10 <sup>d</sup>	82
27	CF <sub>3</sub>	Inh	2.4	89
28	<i>t</i> -Bu		not determined <sup>e</sup>	
29	F	Act	3.8	<10
30	Cl		inactive	
31	Me	Inh	>10 <sup>d</sup>	44
32	OEt	Inh	7.1	98
33	O( <i>n</i> -Pr)	Inh	4.3	95
34	O( <i>i</i> -Pr)	Inh	5.1	92
35	OCH <sub>2</sub> ( <i>c</i> -Pr)	Inh	7.5	59
36	—		inactive	

<sup>a</sup>Inh = inhibitor; Act = activator; NA = not active<sup>b</sup>CRC from T1<sup>+</sup> flux assay in HEK-293 cells expressing WT Slack<sup>c</sup>Amplitude of response in the presence of 30 μM test compound as a percentage of the maximum response for VU0606170 (inhibitors) or loxapine (activators)<sup>d</sup>CRC does not plateau within the concentration range tested<sup>e</sup>Compound appears to be a weak inhibitor/inactive at high concentrations and weak activator at low concentrations

Table 3.

Western ring and linker 1 analogs

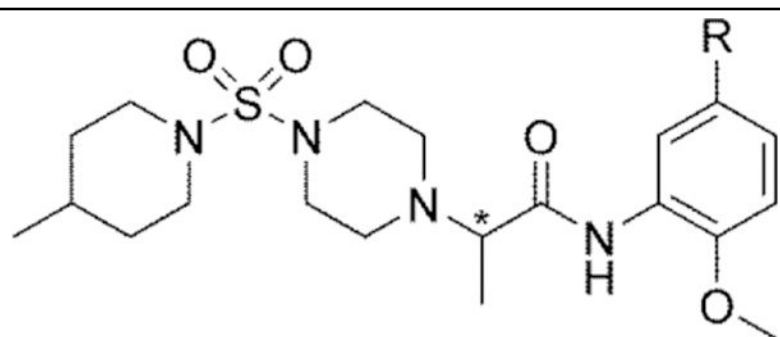


No.	R	Mode <sup>a</sup>	IC <sub>50</sub> / EC <sub>50</sub> (μM) <sup>b</sup>	Efficacy (%) <sup>b,c</sup>
43	piperidin-1-yl		inactive	
44	4-morpholino		inactive	
45	cyclohexyl		inactive	
46	phenyl	Inh	1.1	32
47	4-methylphenyl		inactive	
48	4-chlorophenyl	Inh	2.3	16
50	3,3-difluoropyrrolidin-1-yl	Act	>10 <sup>d</sup>	<10
51	piperidin-1-yl	Act	>10 <sup>d</sup>	10
52	4-propylpiperidin-1-yl	Inh	>10 <sup>d</sup>	58
53	4-isopropylpiperidin-1-yl		not determined <sup>e</sup>	
54	4,4-dimethylpiperidin-1-yl	Act	9.0	23
55	azepan-1-yl	Act	>10 <sup>d</sup>	17

<sup>a</sup> Inh = inhibitor; Act = activator; NA = not active<sup>b</sup> CRC from TI<sup>+</sup> flux assay in HEK-293 cells expressing WT Slack<sup>c</sup> Amplitude of response in the presence of 30 μM test compound as a percentage of the maximum response for VU0606170 (inhibitors) or loxapine (activators)<sup>d</sup> CRC does not plateau within the concentration range tested<sup>e</sup> Compound appears to be a weak inhibitor/inactive at high concentrations and weak activator at low concentrations

Table 4.

Methylated linker 2 analogs



No.	*	R	Mode <sup>a</sup>	IC <sub>50</sub> / EC <sub>50</sub> (μM) <sup>b</sup>	Efficacy (%) <sup>b,c</sup>
60	<i>S</i>	Cl	Inh	4.4	93
61	<i>S</i>	CF <sub>3</sub>	Inh	3.4	95
62	<i>R</i>	Cl	Inh	4.9	98
63	<i>R</i>	CF <sub>3</sub>	Inh	3.5	100

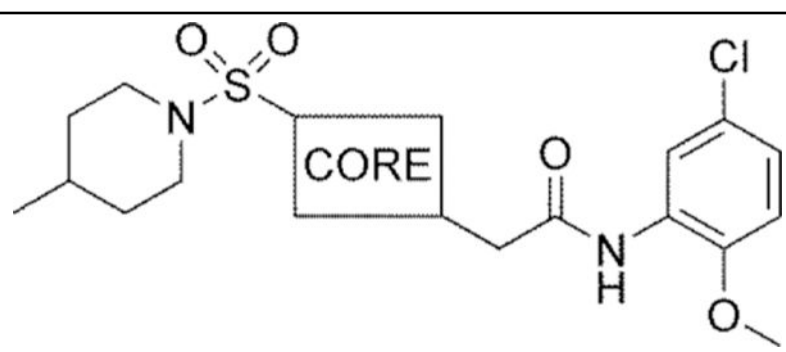
<sup>a</sup>Inh = inhibitor; Act = activator; NA = not active

<sup>b</sup>CRC from TI<sup>+</sup> flux assay in HEK-293 cells expressing WT Slack

<sup>c</sup>Amplitude of response in the presence of 30 μM test compound as a percentage of the maximum response for VU0606170

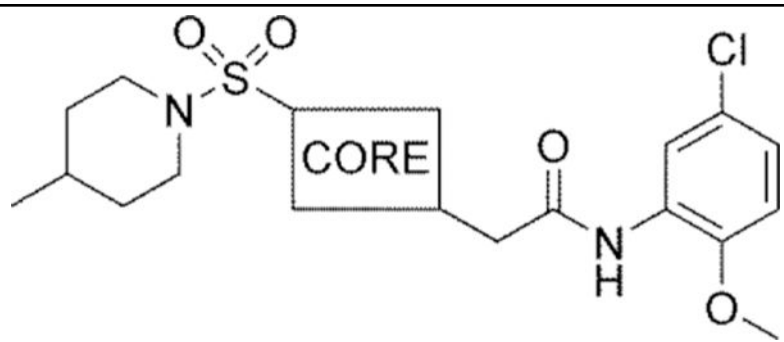
**Table 5.**

Core analogs



No.	CORE	Mode <sup>a</sup>	IC <sub>50</sub> / EC <sub>50</sub> (μM) <sup>b</sup>	Efficacy (%) <sup>b,c</sup>
68		Inh	>10 <sup>d</sup>	20
86		Inh	13	58
71		Inh	3.5	93
87		Inh	2.4	101
81		Inh	>10 <sup>d</sup>	103
85		Act	9.3	25
88		Act	>10 <sup>d</sup>	17
89		Act	10	32





No.	CORE	Mode <sup>a</sup>	IC <sub>50</sub> / EC <sub>50</sub> (μM) <sup>b</sup>	Efficacy (%) <sup>b,c</sup>
90		Inh	>10 <sup>d</sup>	69
91			inactive	
92		Inh	6.2	106

<sup>a</sup>Inh = inhibitor; Act = activator; NA = not active

<sup>b</sup>CRC from Tl<sup>+</sup> flux assay in HEK-293 cells expressing WT Slack

<sup>c</sup>Amplitude of response in the presence of 30 μM test compound as a percentage of the maximum response for VU0606170 (inhibitors) or loxapine (activators)

<sup>d</sup>CRC does not plateau within the concentration range tested

**Table 6.**

Comparison of activity versus WT and A934T Slack for select inhibitors

No.	WT		A934T	
	IC <sub>50</sub> (μM) <sup>a</sup>	Efficacy (%) <sup>a,b</sup>	IC <sub>50</sub> (μM) <sup>a</sup>	Efficacy (%) <sup>a,b</sup>
4	2.4	100	1.4	100
24	4.9	102	2.3	100
27	2.4	89	1.3	88
33	4.3	95	3.1	95
60	4.4	93	2.7	98
61	3.4	95	2.5	96
62	4.9	98	2.9	106
63	3.5	100	2.8	102
71	3.5	93	2.1	94
87	2.4	101	1.1	100

<sup>a</sup>CRC from Tl<sup>+</sup> flux assay in HEK-293 cells expressing either WT or A934T Slack<sup>b</sup>Amplitude of response in the presence of 30 μM test compound as a percentage of the maximum response for VU0606170

**Table 7.**

Slo family selective for select Slack inhibitors

No.	Slick (Slo2.1)		Maxi-K (Slo1 $\alpha$ 1/ $\beta$ 3)	
	IC <sub>50</sub> ( $\mu$ M) <sup>a</sup>	Efficacy (%) <sup>a,b</sup>	IC <sub>50</sub> ( $\mu$ M) <sup>a</sup>	Efficacy (%) <sup>a,b</sup>
<b>4</b>	>10 <sup>c</sup>	35		inactive
<b>27</b>	4.1	29	>10 <sup>c</sup>	36
<b>61</b>	>10 <sup>c</sup>	34		inactive
<b>87</b>	>10 <sup>c</sup>	50	>10 <sup>c</sup>	32

<sup>a</sup> CRC from Tl<sup>+</sup> flux assay in HEK-293 cells expressing either Slick (Slo2.1) or Maxi-K (Slo1  $\alpha$ 1/ $\beta$ 3)

<sup>b</sup> Amplitude of response in the presence of 30  $\mu$ M test compound as a percentage of the maximum response for SKF96365 (Slick) or paxilline (Maxi-K)

<sup>c</sup> CRC does not plateau within the concentration range tested

**Table 8.**

Whole-cell electrophysiology (EP) versus WT and A934T Slack for select inhibitors

No.	WT		A934T	
	IC <sub>50</sub> (μM) <sup>a</sup>	Efficacy (%) <sup>a,b</sup>	IC <sub>50</sub> (μM) <sup>a</sup>	Efficacy (%) <sup>a,b</sup>
<b>4</b>	1.7	100	1.6	100
<b>27</b>	2.3	100	1.1	90
<b>61</b>	1.9	100	1.5	70
<b>87</b>	1.7	100	1.9	100

<sup>a</sup> CRC from whole-cell EP in HEK-293 cells expressing either WT or A934T Slack utilizing an automated patch clamp system<sup>b</sup> Amplitude of response in the presence of 30 μM test compound as a percentage of the maximum response for VU0606170